Temporal changes in anthropogenic seismic noise levels associated with economic and leisure activities during the COVID-19 pandemic

Hiro Nimiya (nimiya.h@aist.go.jp)
National Institute of Advanced Industrial Science and Technology https://orcid.org/0000-0002-4328-6104

Tatsunori Ikeda
Kyushu University

Takeshi Tsuji
Kyushu University

Research Article

Keywords: Seismic noise, Anthropogenic noise, Monitoring, COVID-19

Posted Date: September 17th, 2020

DOI: https://doi.org/10.21203/rs.3.rs-77786/v1

Abstract

Seismic noise of frequencies >1 Hz includes noise that is strongly related to human activities. Reduction in seismic noise during the COVID-19 pandemic has been observed worldwide as restrictions were imposed on numerous human activities to control outbreaks of the virus. In this context, we studied the effect of reduced anthropogenic activities during COVID-19 on the noise levels in the Tokyo metropolitan area, Japan, considering seasonal variation. A significant reduction in noise was observed during the emergency, including that of frequencies >20 Hz, which was associated with school activities. After lifting the state of emergency, noise reverted to previous levels immediately for weekdays, but gradually for Sunday. This was likely because economic activities instantly resumed post-emergency on weekdays; however, most people still continued to avoid non-essential outings on Sunday. We also observed seasonal variation related to school holidays, energy consumption, and industrial activity. Noise levels in the frequency range of 1–5 Hz were found to be related to construction activity, which increased in winter and gradually decreased from 2017. Our findings demonstrate that seismic noise can be used to monitor economic activities and movement of people at a local scale.

Introduction

The ambient seismic noise recorded by seismometers includes microseisms and anthropogenic or cultural noise. While microseisms are caused by the coupling between the ocean and the solid earth at frequencies mostly <1 Hz[1], anthropogenic seismic noise, especially in urban areas, includes seismic signals generated by human activities such as moving people and industrial activities[2–5]. A recent study reported an increase in ambient seismic noise energy in response to an increase in the gross domestic product (GDP), which is associated with the magnitude of human activity[6]. Since an increase in ambient noise energy can be attributed to a wide range of human activities, ambient seismic noise in urban areas tends to be stronger and more complex. For instance, Díaz et al.[5] monitored road traffic and subway trains along an avenue about 150 m away for frequencies >1 Hz (maximum energy between 8–35 Hz) and 20–40 Hz band, respectively. They succeeded in detecting signals generated by various anthropogenic noise including rock concerts, football games, and road traffic. Considering the temporary absence of a specific noise source, Green et al.[7] monitored the ambient seismic noise during a complete shutdown of the subway system during an industrial strike, and found clearly evident reduction for frequencies >25 Hz within 100 m distance but no reduction at a distance of ~600 m from the nearest subway line. Hence, the ambient seismic noise includes various anthropogenic noises depending on the frequency, time, and distance[8,9].

The outbreak of COVID-19 has immensely impacted and imposed restrictions on the routine lives of people all over the world. After the first report of COVID-19, it has spread rapidly and exponentially across the world, with the World Health Organization (WHO) declaring it a pandemic on March 13, 2020[10]. Many countries, including China and Italy, went into lockdown for several weeks to contain major outbreaks of

COVID-19. Although lockdown restrictions were effective in containing the virus' spread, a second or third wave of COVID-19 is a cause for concern. The daily life would change across the world under the outbreak of COVID-19[11]. The large-scale restrictions on human activities during the pandemic also presented a rare opportunity to clearly distinguish anthropogenic seismic noise from ambient seismic noise. Poli et al.[12] and Xiao et al.[13] compared ambient seismic noise levels before and during the pandemic-related lockdown by using continuous seismic records for Italy and China, and observed a clear decrease in noise level during the lockdown. Poli et al.[12] found that the noise level significantly reduced in the frequency band 1–10 Hz. For China, the decrease in noise level was much larger than that for Italy[13]. Xiao et al.[13] inferred that this was caused by the difference in the strictness of enforcing restrictions by the governments of the two countries. Reduction of up to 50% in the noise level in the frequency range 4–14 Hz up to 50 % were observed world over[14]. While the reduction was highest in populated areas, the seismic quiescence extended for several kilometers. At the local scale, continuous fiber-optic distributed acoustic sensing recordings showed a spatial reduction in noise level with a COVID-19 response[15]. A 50% decrease in vehicular noise was observed in one commuter sector immediately following the order to stay indoors, even though traffic near hospitals persisted.

Since the first case was reported on January 28, 2020, the number of confirmed cases in Japan increased. To prevent the spread of infection certain self-restraint advisories, such as school shutdowns and canceling public events, were issued by the national and local governments. In Tokyo, schools remained closed from March 2 to June 30, 2020. In response to the COVID-19 epidemic, the Japanese government declared a state of emergency in Tokyo from April 7 to May 25, 2020, during which many people voluntarily refrained from going out. On the other hand, trains and road traffic did not stop because economic activities still continued.

Regarding the strictness of government advisories, the declaration of the state of emergency by the Japanese government was not legally binding but was more of an appeal for self-restraint. While most people voluntarily refrained from going out, some people and stores did not follow the advisory. In addition, as most economic activities still continued during the emergency, public transport was also continued like the situation in Italy.

With this background we carried out a study to understand anthropogenic seismic noise and estimate the change in human activities during the COVID-19 pandemic by monitoring temporal changes in the seismic noise level around Tokyo.

Figure 1. Arrangement of MeSO-net. Red and green dots and squares show the MeSO-net stations. Dots and squares indicate the stations located in schools and parks, respectively. Blue and magenta lines indicate highways and railways, respectively.

Data Source and Calculation of Power Spectral Density (PSD)

We used the publicly available, continuous, three-component ground acceleration data recorded by the Metropolitan Seismic Observation Network (MeSO-net). MeSO-net stations have acceleration sensors with a sampling rate of 200 Hz and installed at depths of ~20 m to reduce the influence of anthropogenic noise[16,17]. Around 300 MeSO-net stations are deployed around the metropolitan area, out of which we used data from 118 stations located around Tokyo (Fig, 1). We used the vertical component of the seismic noise from 1 December, 2017 to 31 July, 2020.

To estimate the temporal change in ambient noise before and after the COVID-19 outbreak, we calculated the power spectral density (PSD) following the method of McNamara and Boaz[18]. PSD as a function of time and frequency is an effective tool to visually distinguish different types of seismic noise. We divided the daily data into 5-min segments, and applied demean and detrend to each data segment. After applying 10% cosine taper, we calculated the PSD for each 5-min data segment. In this study, we used the median value of PSD in the specific term (e.g., all day, daytime, or night) as the daily PSDs. We expressed PSD in units of decibels (dB) with respect to 1 $(m^2/s^4)/Hz$ to make it easy to compare with previous or future studies.

Figure 2. Time-series and time-dependent PSDs for five stations (a–e). Left panels: time-series PSD from December 2017 to July 2020. Middle panels: time-dependent PSDs on weekdays and Sunday. Right panel: difference between time-dependent PSDs on weekday and Sunday.

PSDs near dominant specific anthropogenic noise sources

We focused on certain stations located near dominant specific noise sources, such as vehicle traffic, train, or industry. To study their spectral features, we estimated two types of PSD, viz. time-series (daily) PSD, and time-dependent PSD. We estimated PSDs by using the median value of all segments each day and at the same time during a day, respectively (Fig. 2). Time-dependent PSDs were calculated using weekday

data and Sunday data, respectively. Here, we excluded bank holidays and long holidays (New Year holidays: December 27–January 6, summer holidays: August 11–August 16 and consecutive holidays: April 28–May 6).

Station GHGM was the closest to railway line (~60 m) but far from the highway (~1.5 km), while, conversely, station TKNM was the closest to the highway (~90 m) but far from the railway line (~2 km) (Fig. 1). The time-series PSDs at GHGM were expected to include seismic signals generated by the train and showed some belt-shaped anomalies, with clear peaks in the wide frequency range of ~10–20 Hz and a narrow frequency range of ~2–4 Hz (Figure 2a). Energy was high from 5 AM to 1 AM, likely caused by seismic noise from trains, since this corresponded with the time between the first (05:06) and last (00:55) train. Additionally, the difference in PSDs between weekdays and Sundays was clear due to the difference in train schedule.

Station TKNM, where seismic signals generated by vehicular traffic on the highway was expected to be dominant, showed a large PSD in a wide frequency range >1.5 Hz, with maximum energy over 1.5–20 Hz (Fig. 2b). This includes the frequency range 4–10 Hz, where the seismic signal generated by trains was weak. Although PSD decreased above 20 Hz, it still had a substantial energy in the higher frequencies depending on the day and time. The time-dependent PSDs clearly showed high energy during daytime on weekdays and a large difference in energy between weekdays and Sundays in the frequency range <20 Hz (Fig. 2b).

Station JKPM was located in a park in an industrial estate, and was far from both the highway (~2 km) and railway track (~3 km) (Fig. 1). The PSD in the frequency range 1–30 Hz was relatively large, with maximum energy over 1–10 Hz (Fig. 2c). Continuous dominant spike noises of certain specific frequencies were observed for the entire period or specific time. In particular, the spike noise ~48 Hz was dominant. It is likely that this noise was caused by vibrations generated by motors, transformers, inverters, etc., associated with mechanical equipment such as air conditioners and vending machines operating on 50 Hz commercial power supply[19,20]. Indeed, a spike noise of ~50 Hz was observed for other stations. Mechanical equipment in the industrial estate could induce additional spike noises at JKPM. The time-dependent PSD for weekdays showed the dominant energy during daytime in the frequency range <50 Hz. The large difference in energy between weekdays and Sundays was observed for the frequency range ~25–35 Hz and 3–10 Hz. Furthermore, the times when the energy increased (~09:00) and decreased (~18:00), and break times (~10:00, 12:00, and 15:00) was clear. These likely correspond to the working time of industries.

Station MBSM was located far from the highway (~2 km) and railway (~1.5 km) (Fig. 1). It showed a relatively low PSD in the entire period compared to other stations (Fig. 2d). A relatively large PSD occurred at a frequency 2–20 Hz, with a peak at ~3 Hz, and it was dominant on weekdays. For frequency range >20 Hz the energy on weekdays was higher around 8 AM and evening, and the energy on Sunday was higher in the morning. Possibly, these high energies were generated by school activities (e.g., going to school and club activities).

GNZM was located downtown and was close to the highway (~80 m) and subway (~110 m). The time-series PSD showed higher energy over a wide frequency range (2–90 Hz) for the entire period compared with other stations (Fig. 2e). High energy was observed in the frequency range >50 Hz except for late at night. A dominant spike noise ~50 Hz was evident, which could be caused by mechanical equipment, like the signals observed at station JKPM. For frequency range 10–30 Hz, we could observe large PSDs even late at night, similar to the signals observed at the station TKNM. The large difference in energy between weekdays and Sundays was evident for the frequency range <10 Hz from around 3 AM to 5 PM.

Frequency ranges

To simplify the frequency-dependent time-series PSD we defined five frequency classes (1–5, 5–10, 10–20, 20–45, and 55–85 Hz) based on the features of PSD, as described above (Fig. 2). In the lowest frequency range 1–5 Hz, PSD was dominant at all stations and also appeared late at night. Considering the signals observed late at night when trains were not running, we deduced that this was most likely caused by truck traffic for logistics. In the frequency range 5–10 Hz, seismic signals that can be mainly generated by trains were weak, and the difference between weekdays and Sundays was large for the stations TKNM, JKPM, and GNZM. PSD in the frequency range 10–20 Hz was dominant for all of these stations, especially GHGM, TKNM, and GNZM. In the frequency range >20 Hz, PSD was still high, depending on the time. PSD in the frequency range 20–45 Hz was greater than that for 55–85 Hz, although their dominant times were similar. While it is difficult to confirm that this classification was applicable for other stations, we still observed five frequency ranges from five stations located near specific dominant noise sources as described above.

We calculated the average value of noise level at each station for each frequency class by considering day (weekday and Sunday), daytime (7 AM to 5 PM), and nighttime (2 AM to 5 AM) (Fig. 3). We clearly see the high energy around the centers of the considered stations. These correspond to the youngest sediments[21]. The noise level strength likely reflected the ease of shaking or amplification due to soft sediments[22,23]. The energy in the frequency range >20 Hz was much smaller than that for the lower

frequency range. The energy was higher during the daytime and on weekdays compared to nighttime and Sundays[2,5].

Figure 3. Average noise levels calculated by considering the day and time in five different frequency classes.

Temporal changes in relative noise level

To monitor the PSD, we estimated the temporal changes in the relative noise level (R) at each station using the following equation:

$$R(\%) = \frac{PSD_{cur} - PSD_{ref}}{PSD_{ref}} \times 100, \quad (1)$$

PSD_{cur} represents the root of the daily PSD, which was estimated using the median value of all segments during specific time segments. We estimated daytime PSD_{cur} and nighttime PSD_{cur} using segments "7 AM to 5 PM" and "2 AM to 5 AM", respectively. In addition, we classified PSD_{cur} into "Weekday" and "Sunday", and removed bank holidays and around long holidays because the calendar effects were strong. We used the average value of PSD_{cur} as PSD_{ref} at each station in each frequency range. Finally, we estimated four relative noise level changes in five frequency classes.

Figure 4 shows some examples of the weekday temporal changes in relative noise levels at the stations located near specific dominant noise sources (Fig. 1). Reduction in the noise level around school shutdown and the state of emergency at certain stations were clearly evident (red lines in Fig. 4). Notably, the temporal changes varied, depending on the station, time, and frequency class.

At station MBSM noise level for frequency >10 Hz clearly decreased from March to June 2020 during daytime compared to previous levels (Fig. 4d). During the state of emergency, stations GHGM and GNZM showed a larger decrease in noise level in the nighttime than during the daytime (Figs. 4a and 4e). For JKPM the temporal changes in noise level were inconsistent (except for the highest frequency range), particularly during nighttime (Fig. 4c). Station TKNM showed a substantial reduction in nighttime noise from March for the frequency range 20–45 Hz; however, this pattern occurred every year (Fig. 4b). At this station, the reduction in the daytime noise on Sundays was larger than that on weekdays. For GHGM,

energy in the frequency range 5–10 Hz was low (Fig. 2a), but the reduction in noise level during the COVID-19 pandemic was substantial. The changes in noise level due to the pandemic were not necessarily related to dominant sources (e.g., train-induced noise).

Figure 4. Temporal changes in relative noise level. Gray, light blue and orange symbols indicate temporal changes in relative noise level for December 2017–November 2018, December 2018–November 2019 and December 2019–July 2020, respectively. Circles and triangles represent weekdays and Sundays, respectively. Black, blue and red lines indicate the smoothed changes in noise level with a 30-day moving average. X-axis shows the number of days from December 1.

Seasonal effects

Many stations showed a reduction in noise level during the COVID-19 pandemic. However, some showed a reduction every year, and we could not distinguish seasonal effects from the effect of COVID-19 (e.g., nighttime in Fig. 4b). To identify stations where the seasonal variations were consistent and strong, we calculated the correlation coefficient (CC) for annual temporal changes in relative noise levels between December 2017–November 2018 and December 2018–November 2019 using the following equation:

$$CC(y_1, y_2) = \frac{cov(y_1, y_2)}{\sigma_{y_1}\sigma_{y_2}}, \quad (2)$$

where y_1 and y_2 represent the smoothed annual changes in noise level with a 30-day moving average for December 2017–November 2018 and December 2018–November 2019 (Fig. 4), respectively. σ_{y_1} and σ_{y_2} represent the variances of y_1 and y_2, respectively.

Figure 5. Map with correlation coefficients, which were calculated considering the day and time in five different frequency classes. Black star indicates Tokyo station. Black arrows indicate the station in the park with high correlation coefficient (55–85 Hz in panel a).

Assuming that a correlation coefficient ≥0.6 signified significant association, we observed strong and consistent seasonal effects for frequencies >20 Hz (Fig. 5). In the frequency range <20 Hz, there was no strong seasonal effect except for that on Sunday in the daytime in the frequency range 1–5 Hz. Around the Tokyo station (center of the city), we observed a low correlation for weekdays in the daytime for the

frequency range 55–85 Hz. Low correlation can be attributed to weak seasonal effects, irregular local events, and changes in the environment.

Figure 5. Map with correlation coefficients, which were calculated considering the day and time in five different frequency classes. Black star indicates Tokyo station. Black arrows indicate the station in the park with high correlation coefficient (55–85 Hz in panel a).

We defined the annual seasonal change as the mean value of changes from December 2017 to November 2018 and December 2018 to November 2019, and we used only data that showed a correlation coefficient >0.6 (Fig. 6).

The annual seasonal changes for weekdays during daytime for the frequency range >20 Hz showed a clear trend (Fig. 6a), with a large peak (from late November to early March) and two dips (around late March and August). Notably, these dips were not observed for Sundays (Fig. 6b). The two dips coincided with long school holidays (roughly from 25 March to 5 April and from 20 July to 31 August). Therefore, we considered that this noise reduction was caused by the absence of the noise generated by school activities.

Considering seasonal change for the nighttime, we observed a strong seasonal variation for the frequency range 20–45 Hz on both weekdays and Sundays (Fig. 6). This noise increases in summer and winter. Hence, this perturbation likely indicates vibrations generated by mechanical equipment (e.g., air conditioners and water heaters). However, this seasonal change due to mechanical equipment could not be observed at frequencies <20 Hz as the background noise was strong (Fig. 3). In the frequency range <20 Hz, many stations showed high correlations only for daytime on Sundays for frequency range 1–5 Hz (Fig. 6). This seasonal variation showed high energy in winter and low in summer, and it could be masked by other strong noises on weekdays.

Figure 6. Seasonal variation in the relative noise level. Thin lines represent stations which showed high correlation coefficient. Black thick line indicates the median value. The seasonal variations were calculated considering the day and time in five different frequency classes.

Temporal changes in relative noise level during the COVID-19 pandemic

We corrected the temporal change in the relative noise level by deducting the annual seasonal change. The corrected temporal change in the relative noise level from December 2019 to July 2020 clearly decreased after temporary school shutdown (from March 2 to May 31) and declaration of a state of emergency (from April 7 to May 25) to contain the spread of COVID-19 (Fig. 7).

Figure 7. Corrected temporal change in relative noise level. Thin lines represent stations which showed high correlation coefficient. Black thick line indicates the median value. Yellow and pink shaded areas respectively represent the periods of school shutdown and the state of emergency in Tokyo. The corrected temporal changes were calculated by considering the day and time for five different frequency classes.

We could clearly see two reductions in noise level on weekdays for daytime in the frequency range >20 Hz (Fig. 7a). These reductions started following the school shutdown and declaration of the state of emergency. Before declaration of emergency the noise level recovered slightly. This period corresponded to normal school holidays. The noise level during school shutdown was similar to that during school holidays. During the state of emergency, the noise level decreased significantly. After the state of emergency was lifted, the noise level immediately recovered to the level before 2020; furthermore, it increased more than the usual level from July.

Focusing on nighttime, we could clearly detect the noise reduction during emergency for the frequency range 5–20 Hz, especially on Sundays, although the number of stations showing high correlation coefficient was limited.

The noise level gradually decreased after school shutdown for Sunday in the daytime in all frequency ranges, even for school holidays. Interestingly, the daytime noise level on Sunday did not immediately recover like that on weekdays, after emergency was lifted, and recovered gradually until the beginning of July.

Discussion And Conclusions

Using continuous seismic data recorded by the MeSO-net, we monitored the change in the seismic noise level around Tokyo. The stations located near specific dominant noise sources showed different features reflecting local seismic signals. Based on these characteristics we defined five frequency classes, and classified the average noise level at each station in these. Even with anthropogenic seismic noise, the

averaged noise level strongly reflected the ease of shaking or the amplification due to the soft sediments[21–23]. McNamara and Buland[3] observed the strongest noise levels in the frequency range >1 Hz due to the large human population in the United States, however, at the scale of our study, the geological effect (i.e., soft sediments) was larger.

We estimated the temporal changes in the relative noise level, and recorded seasonal effects. In the frequency range >20 Hz the noise level showed significant reduction related to the school holidays on weekdays in the daytime. To confirm this seasonal effect, we estimated seasonal change and corrected for changes in noise level in the park, although the number of stations that showed a high correlation coefficient in the park was limited (Figure 8). The stations in the park did not show a seasonal effect related to the school holidays or a sudden reduction associated with school shutdown. Anthropogenic noise in the frequency range >20 Hz was generated by local concentrated human activities such as school activities. As MeSO-net stations are mostly established in schools, the seasonal variations were strongly related to the school holidays.

Figure 8. Weekday corrected and seasonal change in the noise level in the park in the frequency range of 55–85 Hz. Thin blue and red lines respectively represent the seasonal and corrected changes. Black thick dashed and solid line indicates the median value of the seasonal and corrected changes, respectively. Yellow and pink shaded areas respectively represent the periods of school shutdown and the state of emergency in Tokyo.

Furthermore, we observed strong seasonal variation in the frequency range 20–45 Hz for the nighttime. We observed that noise levels increased in summer and winter, possibly due to the vibrations generated by mechanical equipment, and could be ascribed to air-conditioning units at a frequency of 25 Hz[22]. According to the monthly maximum electric power consumption data provided by the Tokyo Electric Power Company Holdings (retrieved 27 August 2020 from https://www.tepco.co.jp/corporateinfo/illustrated/power-demand/peak-demand-monthly-j.html), the electric power consumption increases in summer and winter due to higher consumption of energy in summer and winter, and machinery operations with electrical motors and gearboxes generates more seismic noise[20].

We observed a reduction following the school shutdown and the largest reduction during the state of emergency. During the emergency, in addition to the school shutdown, most of the educational and recreational facilities except for medical facilities, public transport, and factories were ordered to close

down; therefore, noise decreased more significantly than during the school shutdown. After the state of emergency was lifted, the noise level immediately recovered for weekdays. In contrast, it recovered gradually for Sundays. The weekday noise level strongly reflected the effects of the state of emergency, but the Sunday noise level likely reflected the concern of the people about the COVID-19 as most people continued to avoid non-essential outings even after emergency was lifted. Compared to other countries[12–15,24], our results showed a higher reduction for the higher frequency range noise as MeSO-net stations are located in schools and the noise related to school activities is dominant. At frequencies <20 Hz, the reduction in the noise levels was unclear compared to those for higher frequencies because the number of stations that showed a high correlation coefficient was limited.

The noise level at lower frequencies was inconsistent in our study area and the correlation coefficient was low. Hence, it was difficult to evaluate the reduction in noise level due to COVID-19 accurately, although we observed a reduction in the noise level at certain stations. We considered that seismic noise at frequencies <20 Hz, which correlated with GDP[6], was temporarily dominant and fluctuated significantly, weakening the correlation coefficient, and thus masking the effect of COVID-19. Because the MeSO-net stations are distributed in the capital of Japan, where local events (e.g., construction) were conducted even at night, thereby potentially affecting the noise level. At station TKNM, we observed a sudden increase in noise level from June 2018, especially in the daytime for <10 Hz. This change can be attributed to an increase in the number of vehicles on the highway, because an extension of the highway was built near TKNM in June 2018. We can see some sudden changes in noise level at other stations, which could also reflect local events.

Many stations showed high correlation coefficients only for Sundays during daytime in the frequency range of 1–5 Hz. We observed seasonal variations, which increased in winter and decreased in summer, and the reduction of the noise level during the state of emergency. We considered that these variations in the frequency range of 1–5 Hz were related to construction activities. To confirm this, we estimated the average temporal change of the noise level by using the median value of all stations and compared them to the index of construction industry activity given by the Ministry of Economy, Trade and Industry: indices of all industry activities (retrieved 1 September, 2020 from https://www.meti.go.jp/statistics/tyo/zenkatu/index.html) (Fig. 9). The reference of the index of construction industry activity was the mean value of that in 2010. This index reflects the production activity of the construction industry from the supply side. The seasonal index (blue line in Fig. 9) was calculated using X-12-ARIMA developed by the U.S. Department of Commerce. The seasonally adjusted index (green line in Fig. 9) was calculated by removing seasonal effects to compare the monthly data easily.

Figure 9. Comparison between temporal change of the noise level and indices of construction industry activity. Black solid and gray dashed lines indicate averaged temporal change of the noise level of all stations in the frequency range of 1–5 Hz in the daytime on weekday and Sunday, respectively. Blue and green lines indicate seasonal index and seasonally adjusted index of construction industry activity, respectively.

Although the seismic noise level includes the effects of many kinds of sources such as traffic, trains, and rivers[25–28], the trend of the temporal change of noise level in the frequency range of 1–5 Hz roughly followed the seasonal index of construction industry activity. The seasonally adjusted index decreased from April 2017 and the noise level clearly reflected this long-term reduction. We found that the average seismic noise level was strongly related to economic activities, especially construction industry activity. This suggests the possibility of monitoring economic activity in the city[6]. In addition, we could monitor the movement of people in a local area by using high-frequency seismic noise. It is suggested to monitor social isolation and the number of vehicles using seismic noise[15,24]. Although the global positioning system (GPS) is one of the most accurate ways to monitor the movement of people, it has recently become difficult to use the data because of privacy issues.

Furthermore, recently, it has become possible to use these anthropogenic noises for the visualization of near-surface structures since the recent development of permanent high-quality seismic networks and the development of techniques. Anthropogenic seismic noises, such as traffic and trains, were used to extract shear, compressional, or surface waves propagating between pairs of stations by computing cross-correlation for visualization or monitoring[29,30]. Identifying dominant anthropogenic noise helps explore geophysics using passive seismic noise. Studying anthropogenic seismic noise is an efficient way to characterize and monitor specific human activities and to visualize underground structures.

Declarations

Availability of data and materials

MeSO-net data are available at the Hi-net website (https://www.hinet.bosai.go.jp/?LANG=en). The index of construction industry activity was given by the Ministry of Economy, Trade and Industry: indices of all industry activities (https://www.meti.go.jp/statistics/tyo/zenkatu/index.html).

Competing interests

The authors have no competing interests to declare.

Funding

This work was supported by JSPS KAKENHI, Grant Numbers JP19K23544, JP20K04133 and JP20H01997.

Authors' contributions

H.N., T.I., and T.T. contributed toward the conception of this study. H.N. analyzed data and drafted the manuscript. All authors interpreted the results, contributed to the revision and approved the final version of the manuscript.

Acknowledgments

We are grateful to the National Research Institute for Earth Science and Disaster Resilience (NIED) and Earthquake Research Institute, University of Tokyo, for providing seismic data recorded by the MeSO-net.

References

1. Longuet-Higgins, M. S. A theory of the origin of microseisms. *Philos. Trans. R. Soc. London* **243**, 1–35 (1950).
2. Groos, J. C. & Ritter, J. R. R. Time domain classification and quantification of seismic noise in an urban environment. *Geophys. J. Int.* (2009). doi:10.1111/j.1365-246X.2009.04343.x
3. McNamara, D. E. & Buland, R. P. Ambiente noise levels in the continental United States. *Bull. Seismol. Soc. Am.* (2004). doi:10.1785/012003001
4. Larose, E. *et al.* Environmental seismology: What can we learn on earth surface processes with ambient noise? *Journal of Applied Geophysics* (2015). doi:10.1016/j.jappgeo.2015.02.001
5. Díaz, J., Ruiz, M., Sánchez-Pastor, P. S. & Romero, P. Urban Seismology: On the origin of earth vibrations within a city. *Sci. Rep.* **7**, 1–11 (2017).
6. Hong, T.-K., Lee, J., Lee, G., Lee, J. & Park, S. Correlation between Ambient Seismic Noises and Economic Growth. *Seismol. Res. Lett.* (2020). doi:10.1785/0220190369
7. Green, D. N. & Bowers, D. Seismic raves: Tremor observations from an electronic dance music festival. *Seismol. Res. Lett.* (2008). doi:10.1785/gssrl.79.4.546

8. Riahi, N. & Gerstoft, P. The seismic traffic footprint: Tracking trains, aircraft, and cars seismically. *Geophys. Res. Lett.* (2015). doi:10.1002/2015GL063558
9. Kuzma, H. A. *et al.* Vehicle traffic as a source for near-surface passive seismic imaging. in *Symposium on the Application of Geophysics to Engineering and Environmental Problems 2009* 609–615 (2009).
10. Sohrabi, C. *et al.* World Health Organization declares global emergency: A review of the 2019 novel coronavirus (COVID-19). *International Journal of Surgery* (2020). doi:10.1016/j.ijsu.2020.02.034
11. Gössling, S., Scott, D. & Hall, C. M. Pandemics, tourism and global change: a rapid assessment of COVID-19. *J. Sustain. Tour.* (2020). doi:10.1080/09669582.2020.1758708
12. Poli, P., Boaga, J., Molinari, I., Cascone, V. & Boschi, L. The 2020 coronavirus lockdown and seismic monitoring of anthropic activities in Northern Italy. *Sci. Rep.* (2020). doi:10.1038/s41598-020-66368-0
13. Xiao, H., Eilon, Z. C., Ji, C. & Tanimoto, T. COVID-19 Societal Response Captured by Seismic Noise in China and Italy. *Seismol. Res. Lett.* (2020). doi:10.1785/0220200147
14. Lecocq, T. *et al.* Global quieting of high-frequency seismic noise due to COVID-19 pandemic lockdown measures. *Science (80-.).* (2020). doi:10.1126/science.abd2438
15. Lindsey, N. J. *et al.* City-scale dark fiber DAS measurements of infrastructure use during the COVID-19 pandemic. *Geophys. Res. Lett.* (2020). doi:10.1029/2020gl089931
16. Sakai, S. & Hirata, N. Distribution of the Metropolitan Seismic Observation network. *Bull. Earthq. Res. Institute, Univ. Tokyo* **84**, 57–69 (2009).
17. Kasahara, K. *et al.* Development of the Metropolitan Seismic Observation Network (MeSO-net) for detection of mega-thrust beneath Tokyo metropolitan area. *Bull. Earthq. Res. Institute, Univ. Tokyo* **84**, 71–88 (2009).
18. McNamara, D. E. & Boaz, R. I. *Visualization of the seismic ambient noise spectrum in Seismic Ambient Noise*. *Cambridge University Press* (2019).
19. Kawakita, Y. & Sakai, S. Various Types of Noise in MeSO-net. *Bull. Earthq. Res. Institute, Univ. Tokyo* **84**, 127–139 (2009).
20. Kar, C. & Mohanty, A. R. Monitoring gear vibrations through motor current signature analysis and wavelet transform. *Mech. Syst. Signal Process.* (2006). doi:10.1016/j.ymssp.2004.07.006
21. Komatsubara, J. Basal topography of the latest Pleistocene to Holocene incised valley fills beneath the Arakawa Lowland, Kanto Plain, Japan. *Bull. Geol. Surv. Japan* **65**, 85–95 (2014).
22. Green, D. N., Bastow, I. D., Dashwood, B. & Nippress, S. E. J. Characterizing broadband seismic noise in Central London. *Seismol. Res. Lett.* (2017). doi:10.1785/0220160128
23. Su, F. *et al.* The relation between site amplification factor and surficial geology in central California. *Bull. - Seismol. Soc. Am.* (1992). doi:10.1016/0148-9062(92)91630-n
24. Dias, F. L. *et al.* Using Seismic Noise Levels to Monitor Social Isolation: An Example from Rio de Janeiro, Brazil. *Geophys. Res. Lett.* (2020). doi:10.1029/2020GL088748

25. Burtin, A., Bollinger, L., Vergne, J., Cattin, R. & Nábělek, J. L. Spectral analysis of seismic noise induced by rivers: A new tool to monitor spatiotemporal changes in stream hydrodynamics. *J. Geophys. Res. Solid Earth* (2008). doi:10.1029/2007JB005034
26. Inbal, A. *et al.* Sources of long-range anthropogenic noise in southern California and implications for tectonic tremor detection. *Bull. Seismol. Soc. Am.* (2018). doi:10.1785/0120180130
27. Fuchs, F. & Bokelmann, G. Equidistant spectral lines in train vibrations. *Seismol. Res. Lett.* (2018). doi:10.1785/0220170092
28. Bokelmann, G. H. R. & Baisch, S. Nature of Narrow-Band Signals at 2.083 Hz. *Bull. Seismol. Soc. Am.* (1999).
29. Nakata, N., Snieder, R., Tsuji, T., Larner, K. & Matsuoka, T. Shear wave imaging from traffic noise using seismic interferometry by cross-coherence. *Geophysics* (2011). doi:10.1190/geo2010-0188.1
30. Brenguier, F. *et al.* Train Traffic as a Powerful Noise Source for Monitoring Active Faults With Seismic Interferometry. *Geophys. Res. Lett.* (2019). doi:10.1029/2019GL083438

Figures

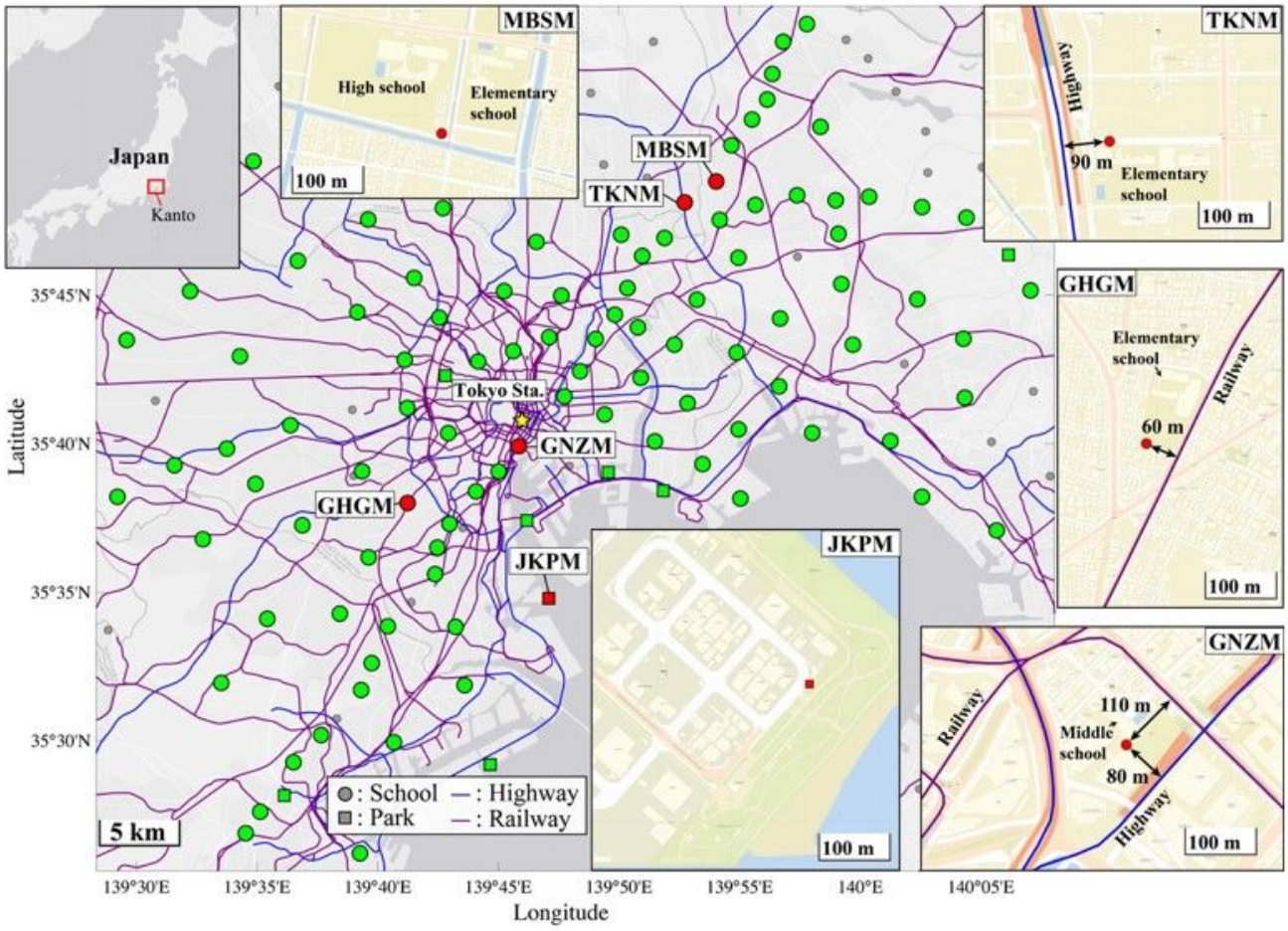

Figure 1

Arrangement of MeSO-net. Red and green dots and squares show the MeSO-net stations. Dots and squares indicate the stations located in schools and parks, respectively. Blue and magenta lines indicate highways and railways, respectively.

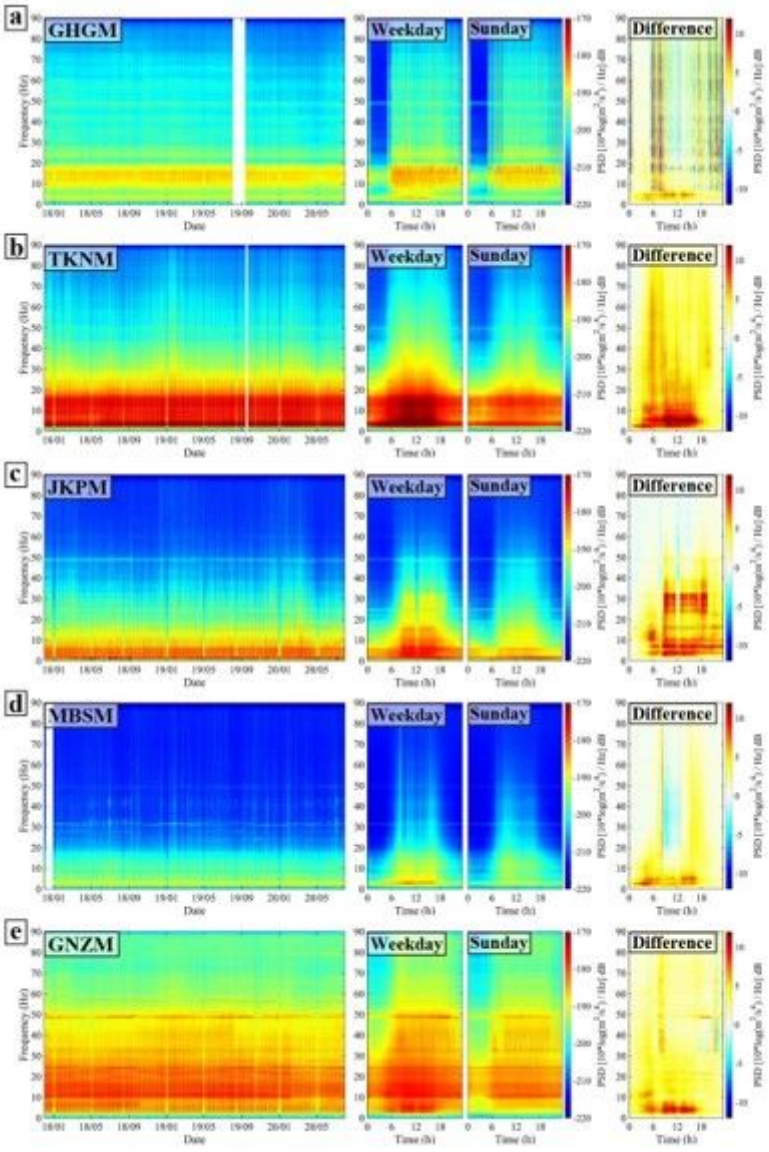

Figure 2

Time-series and time-dependent PSDs for five stations (a–e). Left panels: time-series PSD from December 2017 to July 2020. Middle panels: time-dependent PSDs on weekdays and Sunday. Right panel: difference between time-dependent PSDs on weekday and Sunday.

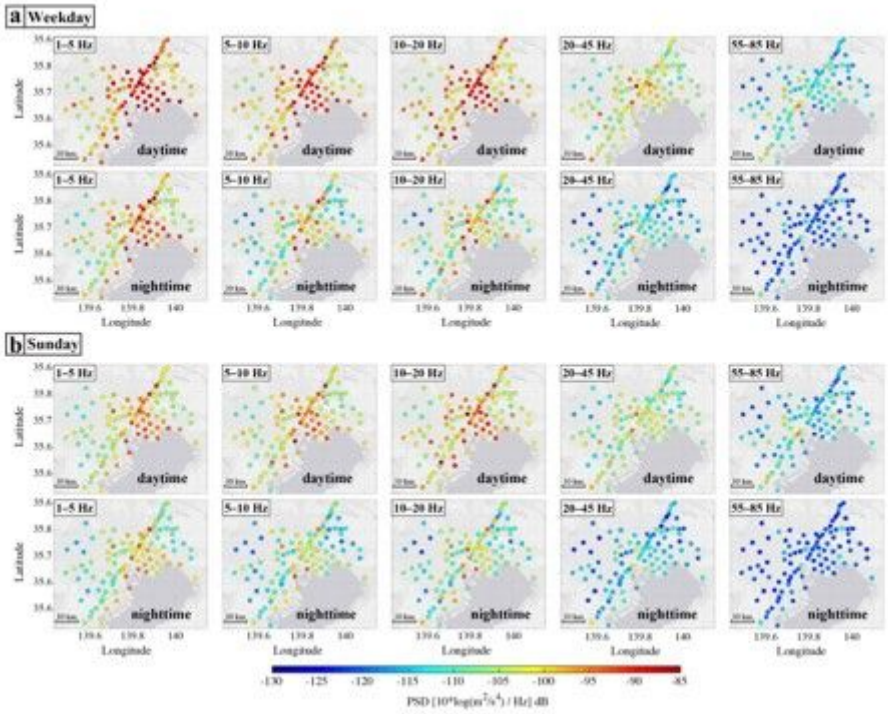

Figure 3

Average noise levels calculated by considering the day and time in five different frequency classes.

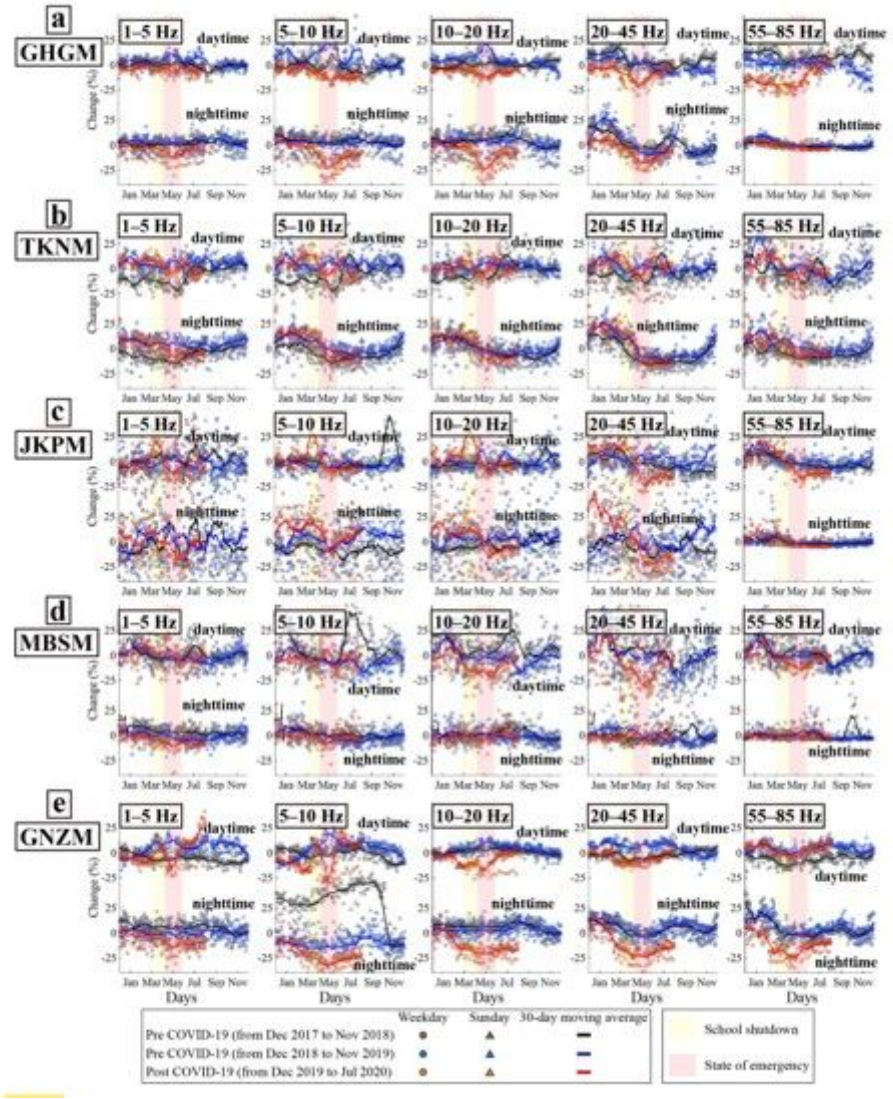

Figure 4

Temporal changes in relative noise level. Gray, light blue and orange symbols indicate temporal changes in relative noise level for December 2017–November 2018, December 2018–November 2019 and December 2019–July 2020, respectively. Circles and triangles represent weekdays and Sundays, respectively. Black, blue and red lines indicate the smoothed changes in noise level with a 30-day moving average. X-axis shows the number of days from December 1.

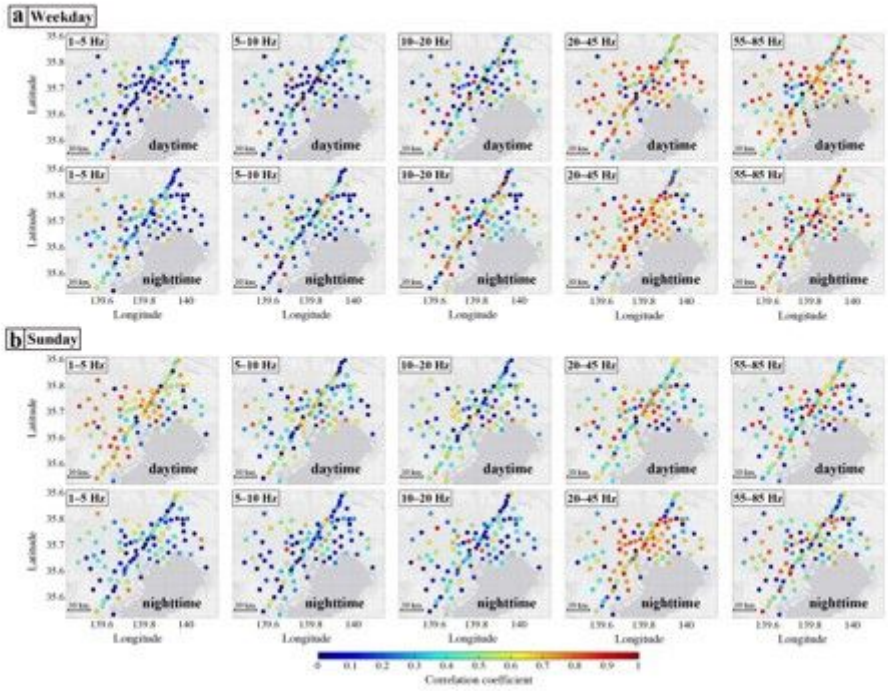

Figure 5

Map with correlation coefficients, which were calculated considering the day and time in five different frequency classes. Black star indicates Tokyo station. Black arrows indicate the station in the park with high correlation coefficient (55–85 Hz in panel a).

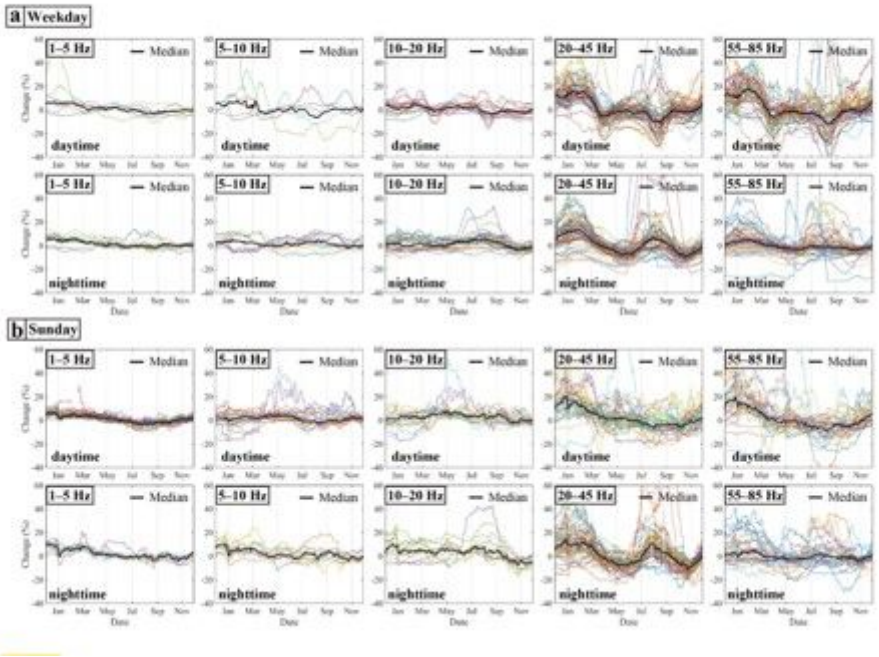

Figure 6

Seasonal variation in the relative noise level. Thin lines represent stations which showed high correlation coefficient. Black thick line indicates the median value. The seasonal variations were calculated considering the day and time in five different frequency classes.

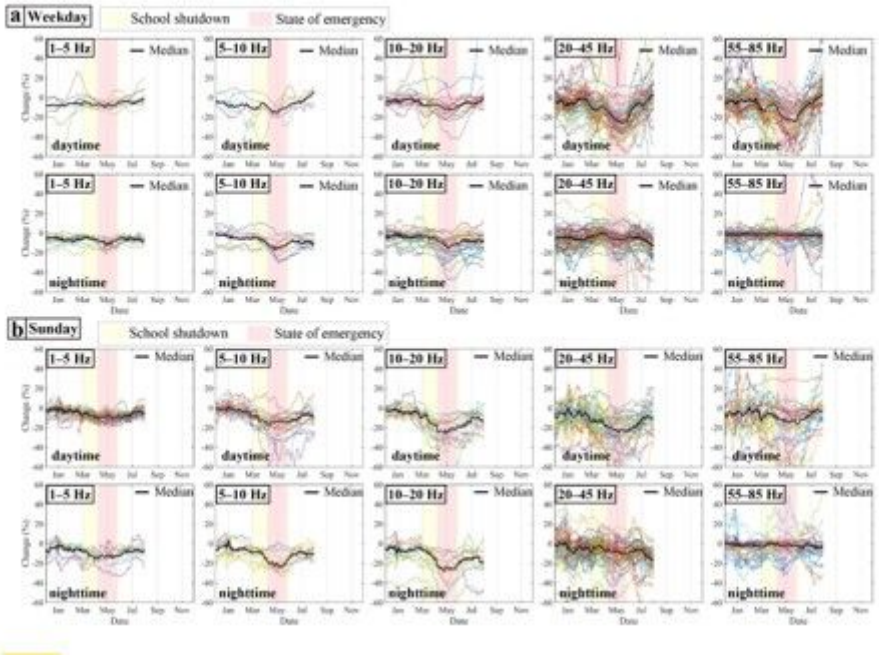

Figure 7

Corrected temporal change in relative noise level. Thin lines represent stations which showed high correlation coefficient. Black thick line indicates the median value. Yellow and pink shaded areas respectively represent the periods of school shutdown and the state of emergency in Tokyo. The corrected temporal changes were calculated by considering the day and time for five different frequency classes.

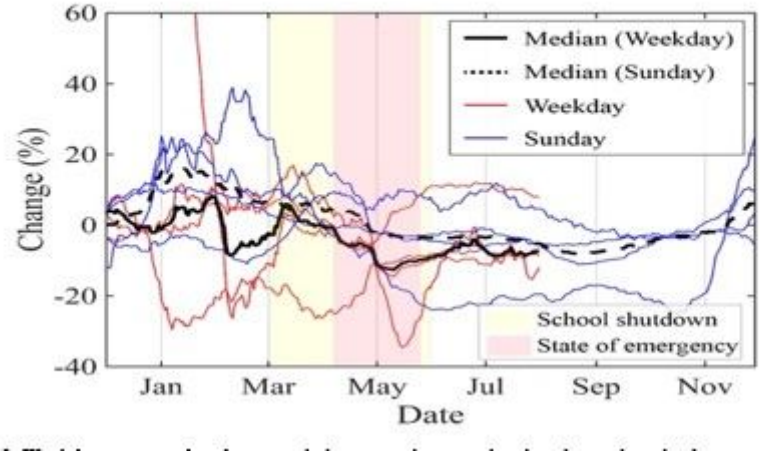

Figure 8

Weekday corrected and seasonal change in the noise level in the park in the frequency range of 55–85 Hz. Thin blue and red lines respectively represent the seasonal and corrected changes. Black thick dashed and solid line indicates the median value of the seasonal and corrected changes, respectively. Yellow and pink shaded areas respectively represent the periods of school shutdown and the state of emergency in Tokyo.

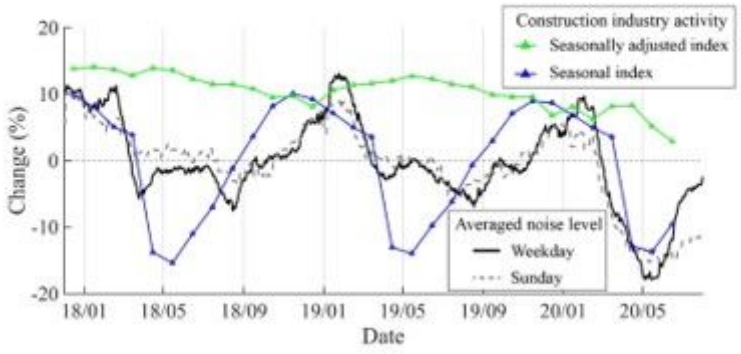

Figure 9

Comparison between temporal change of the noise level and indices of construction industry activity. Black solid and gray dashed lines indicate averaged temporal change of the noise level of all stations in the frequency range of 1–5 Hz in the daytime on weekday and Sunday, respectively. Blue and green lines indicate seasonal index and seasonally adjusted index of construction industry activity, respectively.